# Asymmetric exchange bias training effect in spin glass (FeAu)/FeNi bilayers*

Rui Wen-Bin(芮文彬)[a], He Mao-Cheng(何茂诚)[a], You Biao(游 彪)[a], Shi Zhong(时 钟)[b], Zhou Shi-Ming(周仕明)[b], Xiao Ming-Wen(肖明文)[a], Gao Yuan(高 远)[a], Zhang Wei(张 维)[a], Sun Li(孙 力)[c], and Du Jun(杜 军)[a]†

[a] National Laboratory of Solid State Microstructures and Department of Physics, Nanjing University, Nanjing 210093, China
[b] Department of Physics, Tongji University, Shanghai 200092, China
[c] Department of Mechanical Engineering and Texas Center for Superconductivity (TcSUH), University of Houston, Houston, TX 77204, USA

(Received 9 May 2014; revised manuscript received 7 June 2014; published online 10 August 2014)

A significant exchange bias (EB) training effect has been observed in sputter deposited FeAu/FeNi bilayers, wherein the exchange field ($H_E$) exhibits a special sign-changeable temperature dependence. Very interestingly, despite the absence of multiple easy axes in the FeAu spin glass (SG) layer, $H_E$ drops abruptly between the first and second magnetic cycles, which is followed by a more gradual continuous change in the subsequent cycles. This training behavior cannot be described by the empirical $n^{-1/2}$ law because of the asymmetric magnetization reversal processes. We propose modifying Binek's model to include the asymmetric changes of the pinning SG spins at the descending and ascending branches. This new model successfully describes the EB training effect in FeAu/FeNi bilayers.

**Keywords:** exchange bias, training effect, spin glass

**PACS:** 75.70.Cn, 75.50.Lk, 75.60.–d **DOI:** 10.1088/1674-1056/23/10/107502

## 1. Introduction

The exchange bias (EB) training effect in ferromagnetic/antiferromagnetic (FM/AFM) bilayers (i.e. reductions of both exchange field ($H_E$) and coercivity ($H_C$) during consecutive magnetic hysteresis ($M$–$H$) loop measurements) has been studied extensively because understanding the phenomenon is a critical part of understanding the intricate physics of EB, and in turn, improving the performance of spintronic devices.[1–12] However, the training effect has not been well understood so far. Thermally driven switching of uncompensated AFM spins leads to gradual reduction of EB.[6,10,13] For many bilayers, the exchange field has been found to obey the empirical $n^{-1/2}$ law. Accordingly, a phenomenological model was proposed based on non-equilibrium thermodynamics by Binek.[10] For some bilayers, however, the pattern if the thermal training effect cannot be explained either by the well-known empirical $n^{-1/2}$ law[14,15] or by the Binek's model. The discrepancy arises from the experimental strategy. Such studies are usually focused on the cycle number ($n$) dependence of $H_E$ and $H_C$. For exchange biased bilayers, however, the changes of the coercive fields during consecutive $M$–$H$ loop measurements may be asymmetric, depending on the magnetization reversal mechanism. It is more revealing to study the $n$ dependence of the coercive fields instead of $H_E$ and $H_C$.

In reports of the athermal effect, the exchange field and coercivity often drop abruptly between the first and second cycles. Since the AFM layers have biaxial anisotropy for most exchange biased systems, the athermal effect was initially explained as a result of AFM spin flop between the multiple easy axes during FM magnetization reversal.[11] Surprisingly, however, it may also come from other sources such as the exchange and dipolar coupling and the spin clusters at the interface, instead of biaxial magnetic anisotropy.[16,17] This discrepancy may arise from the definition of the athermal effect. Indeed, the abrupt change of the exchange field between $n = 1$ and 2 does not obey the empirical $n^{-1/2}$ law. Hence, the athermal training effect was proposed. However, as pointed out above, the empirical law does not consider the asymmetric changes of the coercive fields of two branches during the training effect. Therefore, the definition of the athermal effect may not be sufficiently rigorous. In order to reveal the mechanism of the training effect, a pinning layer without biaxial magnetic anisotropy should be employed.

Recently, Mannan Ali *et al.*[18] and Fu-Te Yuan *et al.*[19] demonstrated independently that EB can also be established by including spin glass (SG) layers. Note that in such totally magnetic-disordered materials, exclusively uniaxial anisotropy can be established after field cooling,[20] and this allows us to study the training mechanism in the absence of biaxial magnetic anisotropy. In this work, we present a detailed study of the thermal training effect that employed FeAu(SG)/FeNi(FM) bilayers. The behavior of the exchange

*Project supported by the National Basic Research Program of China (Grant Nos. 2014CB921101 and 2010CB923401) and the National Natural Science Foundations of China (Grant Nos. 51331004, 11074112, and 11174131).

†Corresponding author. E-mail: jdu@nju.edu.cn

© 2014 Chinese Physical Society and IOP Publishing Ltd 

field cannot be adequately explained by the $n^{-1/2}$ law, even when $n \geq 2$. After considering the fact that magnetization along the descending and ascending branches behaves quite asymmetrically, we propose a modified Binek's model[10] to incorporate the evolution of pinning spins at the ascending and descending branches and use the coercive field to quantify the training effect. Both the continuous, gradual change when $n \geq 2$, and the abrupt change between $n = 1$ and 2 can be explained by the modified model.

## 2. Experimental

A series of multilayers with a stacking sequence of Ta(4 nm)/$Fe_xAu_{(100-x)}$($t$ nm)/FeNi(5 nm)/Ta(2 nm) were deposited on silicon wafers by DC magnetron sputtering at room temperature, where $x$ denotes the composition of Fe and varies from 3.5 at.% to 13.5 at.%. The FeAu layer thickness $t$ varies from 5 nm to 50 nm. FeNi represents the $Fe_{19}Ni_{81}$ being used as the ferromagnetic layer. A 4-nm Ta buffer layer was deposited to promote the SG/FM morphology and a 2-nm Ta capping layer was deposited to prevent oxidation of the samples. The FeAu layers were made by co-sputtering with tilted iron and gold guns. The thickness of the FeNi layer was fixed at 5 nm for all multilayers. Another series of single $Fe_xAu_{(100-x)}$ layers was deposited on Kapton substrates as reference samples for low temperature spin glass characterization using zero-field-cooled (ZFC) and field-cooled (FC) $M$–$T$ measurements. The base pressure for sputtering was better than $7.0\times10^{-6}$ Pa and the working Ar pressure was kept at 0.3 Pa during film deposition. Chemical composition of the FeAu layer was characterized by energy dispersive X-ray spectroscopy (EDX). Magnetic measurements were performed in a SQUID-VSM (Quantum Design) with the $M$–$H$ loops measured with an applied magnetic field (in the range from −5 kOe to 5 kOe, the unit 1 Oe = 7.5775 A·m$^{-1}$) parallel to the film plane after field cooling. In order to obtain accurate values of $H_E$ and $H_C$, care was taken to ensure that the residual magnetic field was smaller than 3 Oe.

## 3. Results and discussion

Figure 1 shows the temperature dependence of $H_E$ and $H_C$ for a Ta(4 nm)/$Fe_{11}Au_{89}$(50 nm)/FeNi(5 nm)/Ta(2 nm) sample, which has been cooled from 300 K to 2 K under a magnetic field of 50 kOe. The inset displays the ZFC and FC $M$–$T$ curves from the reference $Fe_{11}Au_{89}$ film measured with a 50-Oe magnetic field from 5 K to 300 K. Typical spin glass behavior can be observed with a $T_F$ of about 30 K. Since the EB training effect in our samples still existed when $n > 10$, all of the samples were trained to a relatively stable state before determining the $H_E$ and $H_C$ values at each temperature. In Fig. 1, $H_E$ shows a clear sign change near 4 K and $H_E$ and $H_C$ show very similar peaks around 7 K, which are typical features for exchange-biased SG/FM bilayers.[18] This particular sample has a maximum positive $H_E$ of about 18 Oe, which is much larger in magnitude than any previously reported results. (Maximum $H_E$ is normally less than 10 Oe, even when the FM layer is only 2.2 nm, as described in Ref. [18].) This may be due to the cooling field of 50 kOe used in the current experiment, which is much stronger than those ($\leq$ 5 kOe) reported before.[18,19] Our recent studies show that both $H_E$ and $H_C$ are significantly influenced by the cooling field, but that is not the main subject of this work and so it will be discussed elsewhere.[21]

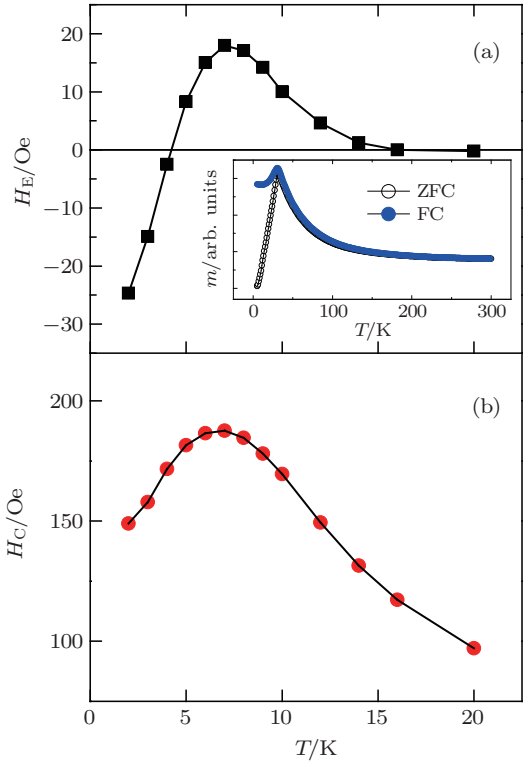



**Fig. 1.** (color online) Temperature dependences of $H_E$ (a) and $H_C$ (b) for a Ta(4 nm)/$Fe_{11}Au_{89}$(50 nm)/FeNi(5 nm)/Ta(2 nm) sample measured between $T = 2$ K and 20 K. The inset compares the zero-field-cooled (ZFC) and the field-cooled (FC) $M$–$T$ curves of a 50-nm $Fe_{11}Au_{89}$ single layered film.

For the current FeAu/FeNi sample, the magnitude of $H_E$ decreases and vanishes at about 16 K, which can be regarded as the exchange bias blocking temperature $T_B$. This value is only about one half of $T_F$, which is much lower than the $T_B$ of conventional FM/AFM bilayers, that is often just a little lower than the AFM Néel temperature $T_N$. The abnormal sign-change temperature dependence of $H_E$ can be explained by the competition between the long range oscillatory RKKY coupling of the spins located deep inside the SG layer and short range direct coupling of those spins close to the interface.[18,19] In contrast, the exchange bias is merely an interfacial effect and the sign of $H_E$ can hardly change in response to temperature variations in conventional FM/AFM bilayers.[22]

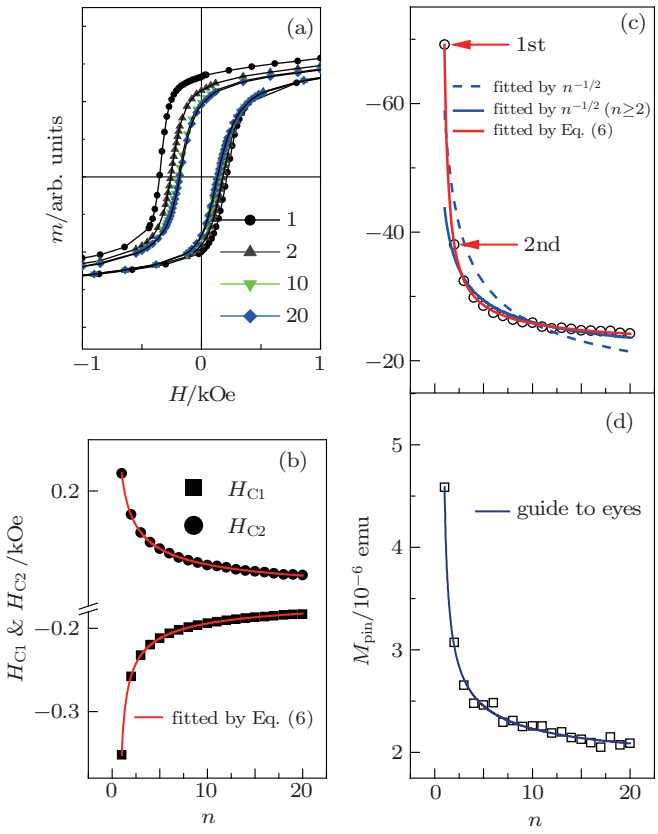



**Fig. 2.** (color online) The $M$–$H$ loops measured in a Ta(4 nm)/$Fe_{11}Au_{89}$(50 nm)/FeNi(5 nm)/Ta(2 nm) sample at $T$ = 2 K at cycle $n$ = 1, 2, 10, 20 (a). The cycle number dependencies of $H_{C1}$ and $H_{C2}$ (b), $H_E$ (c), and $M_{pin}$ (d). The dots and the lines in panels (b) and (c) represent the experimental and fitted results, respectively.

Training behavior is usually characterized by the changes in $H_E$ and $H_C$ versus the magnetic cycle number $n$. Figure 2(a) illustrates the evolution of the $M$–$H$ loops with $n$ = 1, 2, 10, and 20 for the same sample used to obtain Fig. 1. During the consecutive $M$–$H$ loop measurements, the $M$–$H$ loop shrinks from both sides and meanwhile the absolute value of $H_{C1}$ decreases much faster than $H_{C2}$, indicating that the training behavior at the descending and ascending branches is quite asymmetric. The measured $n$ dependence of $H_E$ is summarized in Fig. 2(c). A significant drop in $H_E$ between $n = 1$ and $n = 2$ can be seen, and the training effect remains strong when $n \geq 2$. This differs from the results reported earlier.[18,23] Due to the long-range RKKY interaction in SG/FM bilayers, the pinning spins coupled to the FM layer may extend into the entire SG layer, which may be probed by an ordinary magnetometer. In EB systems, there can be a vertical shift in the $M$–$H$ loops, which results in a difference in the magnitude of saturation magnetization along the cooling field direction ($M_S^+$) and opposite to it ($M_S^-$). The nonzero value of $M_S^+ + M_S^-$ is usually defined as $M_{pin}$.[24] In this present work, $M_S^+$ and $M_S^-$ are the magnetization measured at 5 kOe and −5 kOe, respectively. Although $M_{pin}$ is not a direct measurement of the pinning magnetization in the SG layer, they are closely correlated. The measured $n$ dependence of $M_{pin}$ is shown in Fig. 2(d), where it can be seen that it follows the same trend as $H_E$. This further confirms that the training effect in this SG/FM bilayer originates from the evolution of the pinning SG spins.

We now turn to considering the mechanism of the EB training effect in the SG/FM bilayer. As we mentioned previously, the SG layer by itself is totally magnetic-disordered, so a uniaxial anisotropy can be induced along the field direction after field cooling,[20] and, hence, the Hoffmann mechanism based on the existence of biaxial magnetic anisotropy can be excluded, although a similar significant drop of $H_E$ is observed between the first two cycles. On the other hand, it is widely accepted that the empirical $n^{-1/2}$ law can serve to describe the thermally activated training effect in FM/AFM bilayer systems, and a phenomenological origin has been provided in Binek's approach under the framework of nonequilibrium thermodynamics.[10] Very surprisingly, however, the experimental results obtained here cannot be fitted well by the $n^{-1/2}$ law of $H_E$, regardless of whether the first data point ($n = 1$) is included, as shown by the blue dashed and solid lines in Fig. 2(c). In our understanding, the $n^{-1/2}$ law was deduced without considering the symmetry of the training effect in the ascending and descending branches. In order to get deep insight of the EB training mechanism in a SG/FM bilayer, the asymmetric dependence of $H_{C1}$ and $H_{C2}$ on the cycle number should be considered.

To reveal the phenomenological origin of the EB training effect in such SG/FM bilayers, we propose a modification of Binek's model.[10] Within the framework of this model, we suppose that the EB training effect is essentially generated from the evolution of the pinning SG spins that interact with the FM layer during magnetic cycles. Therefore, the time-dependent pinning SG spins under the influence of alternating FM moment are considered first. Then, a spin glass state with a uniaxial anisotropic axis along the cooling field direction (with an anisotropic energy of $K_{SG}$) is assumed to exist as a cooperative and collective phase below $T_F$.[20] In this model, the uniaxial anisotropy for the soft FM layer is neglected for simplicity. Based on these considerations, the energy per unit area of the SG/FM system can be written as:[25]

$$\begin{aligned} E_{total} &= -\mu_0 H M_{FM} t_{FM} \cos(-\beta) + K_{SG} t_{SG} \sin^2(\beta) \\ &\quad - J_{RKKY} S_{FM} S_{SG}(t) \cos(\beta), \end{aligned} \tag{1}$$

where $H$ is the external magnetic field parallel to the cooling field direction, $M_{FM}$ is FM's saturation magnetization, $t_{FM}$ and $t_{SG}$ are the thicknesses of the FM layer and the SG layer, respectively, $\beta$ is the angle between the external magnetic field and the FM moment, $J_{RKKY}$ defines the exchange coupling strength between the spins in the FM layer, which have a magnetization of $S_{FM}$, and the spins in SG layer, which have a magnetization of $S_{SG}(t)$. It should be emphasized here that

the SG spins that interact with the FM spins are not stable during the $M$–$H$ loop measurements, which is the very reason for the training effect observed in this experiment. The values of $H_{C1}$ and $H_{C2}$ of the $n$-th $M$–$H$ loop obtained from the energy minimum condition are

$$H_{C1}(n) = -\frac{2K_{SG}t_{SG}}{\mu_0 M_{FM} t_{FM}} - \frac{J_{RKKY}S_{FM}}{\mu_0 M_{FM} t_{FM}} S_{SG}^{d}(n),$$
$$H_{C2}(n) = \frac{2K_{SG}t_{SG}}{\mu_0 M_{FM} t_{FM}} - \frac{J_{RKKY}S_{FM}}{\mu_0 M_{FM} t_{FM}} S_{SG}^{a}(n). \quad (2)$$

Here, $S_{SG}^{a}(n)$ and $S_{SG}^{d}(n)$ are the pinning SG magnetization at $H_{C1}(n)$ and $H_{C2}(n)$, respectively. Obviously, $H_{C1}(n)$ and $H_{C2}(n)$ depend linearly on $S_{SG}^{d}(n)$ and $S_{SG}^{a}(n)$, respectively. Thus, defined as

$$H_E(n) = \frac{H_{C1}(n) + H_{C2}(n)}{2}$$

and

$$H_C(n) = \frac{-H_{C1}(n) + H_{C2}(n)}{2},$$

the expressions for $H_E$ and $H_C$ of the $n$-th $M$–$H$ loop can also be obtained. Although the above equations (1) and (2) reveal the relationship between the pinning SG magnetization and $H_E$ or $H_C$ during the training process, it remains unclear exactly how the pinning SG magnetization will change with the cycle number $n$.

Binek[10] proposed a simple analytic approach to describe the exchange bias training effect by considering the damping of AFM interfacial magnetization in FM/AFM bilayers, which is utilized here in describing the SG/FM bilayer simply by replacing the magnetization of AFM spins with SG spins. Because the $M$–$H$ loops were measured continuously in our experiment, the time interval $\Delta t$ between each loop can be neglected. Therefore, the time-dependent pinning SG magnetization can be expressed as $S_{SG}(t)$ for the measurement. With the final equilibrium pinning SG magnetization after training defined as $S_{SG}(\infty)$, the change of pinning SG magnetization $\delta S_{SG}(t)$ can be defined as $S_{SG}(t)$–$S_{SG}(\infty)$ and the change of total free energy $F$ according to Eq. (2) in Ref. [10] can be rewritten as

$$\Delta F = \frac{1}{2} a \delta S_{SG}^{2}(t) + \frac{1}{4} b \delta S_{SG}^{4}(t) + O\left(\delta S_{SG}^{6}(t)\right). \quad (3)$$

Following a procedure similar to the one described in Ref. [10], the evolution of pinning SG magnetization $\xi \dot{S}_{SG}(t) = -b\delta S_{SG}^{3}(t) = -b\left(S_{SG}(t) - S_{SG}(\infty)\right)^3$ can be obtained using the Landau–Khalatinikov (LK) equation:

$$\xi \dot{S}_{SG}(t) = -\frac{\partial \Delta F}{\partial S_{SG}(t)},$$

where $\xi$ is a phenomenological damping constant. Thus, after integration, we can get the expression for $S_{SG}(t)$ as follows:

$$S_{SG}(t) = S_{SG}(\infty) \pm \sqrt{\frac{\xi}{2b}} (t + t_0)^{-1/2}. \quad (4)$$

Here, $t_0$ comes from the integration, representing the initial state of the system. The signs "+" and "−" reflect the amount that $S_{SG}$ decreased or increased, respectively. How the sign is determined will be described below. Because the time interval $\tau$ required for each loop is the same, $t$ in Eq. (4) is proportional to $n$; that is, $t = n\tau$. Therefore, the cycle number dependence of $S_{SG}(n)$ can be described as

$$S_{SG}(n) = S_{SG}(\infty) \pm \sqrt{\frac{\xi}{2b\tau}} (n + n_0)^{-1/2} \quad (5)$$

Like $t_0$ in Eq. (4), $n_0$ is also related to the initial state of the system. The above treatment of discretizing the pinning SG magnetization is the biggest advantage of our model and also the largest difference from Binek's model in Ref. [10]. This treatment enables us to quantify the evolution of the pinning SG magnetization at any position of the $M$–$H$ loop. Hence, for the position of the coercive field at the descending or ascending branch, equation (5) can be rewritten as

$$S_{SG}^{d(a)}(n) = S_{SG}^{d(a)}(\infty) \pm \sqrt{\frac{\xi^{d(a)}}{2b\tau}} \left(n + n_0^{d(a)}\right)^{-1/2},$$

where $\xi^{d(a)}$ are the damping constants for $S_{SG}^{d(a)}(n)$. Then, plugging the expression for $S_{SG}^{d(a)}(n)$ into Eq. (2), the $n$ dependence of $H_{C1}$ and $H_{C2}$ can be described as

$$H_{C1(2)}(n) = H_{C1(2)}(\infty) + k_{1(2)} \left(n + n_0^{1(2)}\right)^{-1/2}. \quad (6)$$

Here,

$$H_{C1}(\infty) = -\frac{2K_{SG}t_{SG}}{\mu_0 M_{FM} t_{FM}} - \frac{J_{RKKY}S_{FM}}{\mu_0 M_{FM} t_{FM}} S_{SG}^{d}(\infty)$$

and

$$H_{C2}(\infty) = \frac{2K_{SG}t_{SG}}{\mu_0 M_{FM} t_{FM}} - \frac{J_{RKKY}S_{FM}}{\mu_0 M_{FM} t_{FM}} S_{SG}^{a}(\infty),$$

and they both represent coercive fields within the limit of infinite loops; $n_0^1$ and $n_0^2$ denote the initial states for the descending and ascending branches respectively; that is,

$$k_1 = \mp \frac{J_{RKKY}S_{FM}}{\mu_0 M_{FM} t_{FM}} \sqrt{\frac{\xi^{d}}{2b\tau}}$$

and

$$k_2 = \mp \frac{J_{RKKY}S_{FM}}{\mu_0 M_{FM} t_{FM}} \sqrt{\frac{\xi^{a}}{2b\tau}}.$$

By fitting the experimental $n$ dependences of $H_{C1}$ and $H_{C2}$ by Eq. (6), one can acquire both the quantity and the sign of $k$. Note that positive (negative) $k$ means the amount of $S_{SG}$ has increased (decreased). According to Eq. (6) and $H_E = (H_{C1} + H_{C2})/2$, one can clearly see that if $n_0^1 \neq n_0^2$ and/or $k_1 \neq k_2$, $H_{C1}$ and $H_{C2}$ will change asymmetrically with $n$ and the empirical $n^{-1/2}$ law does not hold.

To test the validity of the above model, fitting calculations were carried out. Figure 2(b) compares the experimental and calculated results of $H_{C1}$ and $H_{C2}$ as a function of $n$ at $T = 2$ K for the same sample shown in Fig. 1, where a perfect fit described by Eq. (6) can be obtained. Moreover, the $n$ dependence of the fitted $H_E$ can also be calculated according to $H_E = (H_{C1} + H_{C2})/2$. As indicated by the red solid line in Fig. 2(c), it also agrees perfectly with the experimental results. Of course, because $H_C = (-H_{C1} + H_{C2})/2$, the $n$ dependence of $H_C$ can also be perfectly fitted. The corresponding fitting parameters for $H_{C1}$, $H_{C2}$ are listed in Table 1, in which one can clearly see that $k_1$ is negative and $k_2$ is positive, and the absolute value of $k_1$ is larger than that of $k_2$. As mentioned above, a negative $k_1$ means that $S_{SG}$ decreased and thus caused the descending curve to shift rightward, while a positive $k_2$ denotes an increase of $S_{SG}$ and the ascending curve shifting leftward. Therefore, the $M$–$H$ loop shrinks from both sides with the cycles, agreeing well with experimental observations. On the other hand, since $|k| \propto \sqrt{\xi}$, one has $\xi^d > \xi^a$, which agrees with the commonly observed asymmetry of the $M$–$H$ loops in exchange-biased systems. Moreover, since the parameter $\xi$ depicts the damping rate of $S_{SG}$ during the magnetic cycles, it is easy to understand that $|H_{C1}|$ drops faster than $|H_{C2}|$.

**Table 1.** Fitting parameters obtained from Eq. (6) for $H_{C1}$, $H_{C2}$ for a Ta(4 nm)/$Fe_{11}Au_{89}$(50 nm)/FeNi(5 nm)/Ta(2 nm) sample and a Ta(4 nm)/$Fe_8Au_{92}$(50 nm)/FeNi(5 nm)/Ta(2 nm) sample measured at 2 K.

| | $H_{C1}(\infty)$/Oe | $H_{C2}(\infty)$/Oe | $k_1$/Oe | $k_2$/Oe | $n_0^1$ | $n_0^2$ |
|---|---|---|---|---|---|---|
| $Fe_{11}Au_{89}$/FeNi | –155.2 | 113.3 | –118.6 | 91.1 | –0.6 | –0.1 |
| $Fe_8Au_{92}$/FeNi | –104.5 | 50.8 | –61.5 | 77.0 | –0.8 | –0.4 |

In order to convey an intuitive understanding of the reason for the EB training effect in the SG/FM bilayers, a schematic diagram is presented in Fig. 3, which illustrates the evolution of the pinning SG magnetization at the descending branch ($S_{SG}^d$) and the ascending branch ($S_{SG}^a$) for two consecutive $M$–$H$ loops. Before going further, two important issues need to be addressed. First, the reversal of the FM layer magnetization is the key factor that triggers the evolution of pinning SG magnetization. Second, during an $M$–$H$ loop measurement, the decrease of pinning SG magnetization when the FM moment is antiparallel to the pinning direction is larger than the increase when the FM moment is parallel, which is similar to the FM/AFM systems described by LLG equation in Ref. [26]. Therefore, as shown clearly in Fig. 3(b), after the $M$–$H$ loop changes from $n$-th to $(n+1)$-th, the inequation $\Delta S_{SG}^d = S_{SG}^d(n+1) - S_{SG}^d(n) < 0$ is satisfied, which implies a decrease of pinning SG magnetization at the descending branch. Meanwhile, another inequation $\Delta S_{SG}^a = S_{SG}^a(n+1) - S_{SG}^a(n) > 0$ implies an increase in pinning SG magnetization at the ascending branch. This is why $k_1$ ($k_2$) is always negative (positive), and thus shrinkage from both sides in the $M$–$H$ loop is observed. However, the difference between $\Delta S_{SG}^d$ and $\Delta S_{SG}^a$ depends mainly on the absolute values of $k$ because $|k| \propto \sqrt{\xi}$. For the sample displayed in Fig. 2, since $|k_1| > |k_2|$, $|\Delta S_{SG}^d|$ is larger than $|\Delta S_{SG}^a|$.

A much more surprising training effect has been observed at 2 K in another sample, that is, Ta(4 nm)/$Fe_8Au_{92}$(50 nm)/FeNi(5 nm)/Ta(2 nm), after being cooled from 300 K to 2 K under a 70-kOe magnetic field. As shown in Fig. 4(a), although the $M$–$H$ loop still shrinks from both sides in consecutive measurements (not shown here) and $H_E$ also decreases dramatically from $n = 1$ to $n = 2$, $H_E$ increases a little during the subsequent training process. This non-monotonic variation of $H_E$ with $n$ has never been observed in conventional FM/AFM bilayers and certainly cannot be fitted by the empirical $n^{-1/2}$ law. Surprisingly, this abnormal training effect can be perfectly fitted by Eq. (6), as shown in Figs. 4(a) and 4(b), and the fitting parameters are listed in Table 1. In comparison with the sample shown in Fig. 2, although the sign of $k_1$ or $k_2$ remains unchanged, the absolute value of $k_1$ becomes smaller than that of $k_2$, leading to an increase of $H_E$ for $n > 2$. The quite significant difference of EB training behavior may result from the different spin configurations in the FeAu layer at various Fe concentrations. Note that in some newly developed SG-induced EB systems, such as $BiFeO_3$–$Bi_2Fe_4O_9$ nanocomposite,[15] Fe–Ni–B nanostructures,[27] and $BiFeO_3$/NiFe bilayers,[28] the training behavior can all be fitted well by Eq. (6).

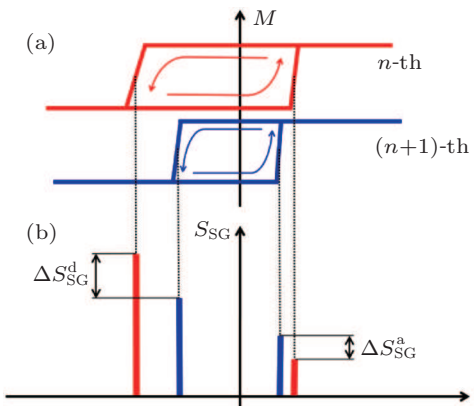



**Fig. 3.** (color online) Schematic illustrations of $M$–$H$ loops of cycle number $n$ and $n+1$ (a) and the pinning SG magnetizations at the coercive fields of the $M$–$H$ loops (b).

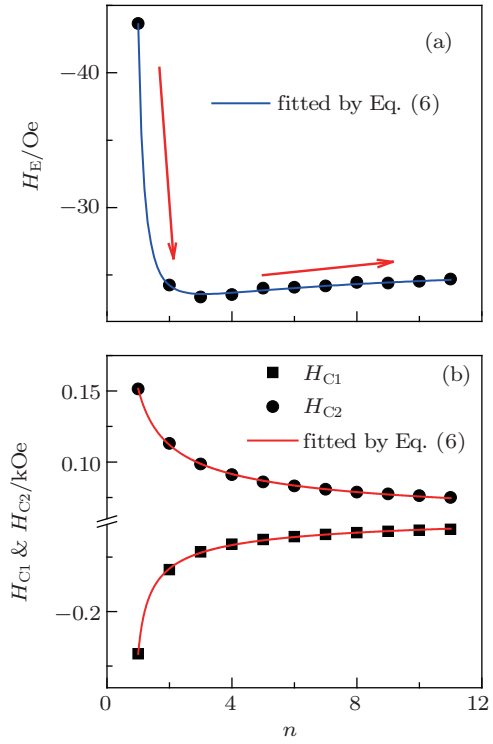



**Fig. 4.** (color online) Cycle number dependence of $H_E$ (a), $H_{C1}$ and $H_{C2}$ (b) for a Ta(4 nm)/$Fe_8Au_{92}$(50 nm)/FeNi(5 nm)/Ta(2 nm) sample. The dots and lines represent the experimental and fitted results, respectively.

## 4. Conclusions

In conclusion, the EB training effect in the FeAu(SG)/FeNi(FM) bilayers has been investigated both experimentally and theoretically. With increasing temperature, a sign-changeable temperature dependence of $H_E$ can be observed, which is due to competition between the long range oscillatory RKKY coupling of the spins inside the SG layer and short range direct coupling from those spins close to the interface. In addition to the gradual change of EB, there is an abrupt change of the exchange field between $n = 1$ and 2, despite the absence of biaxial anisotropy in the spin glass layer. This abnormal training effect cannot be adequately described by the empirical $n^{-1/2}$ law. After considering the asymmetric evolution of pinning SG spins at the descending and ascending branches, both the abrupt change of the EB between $n = 1$ and 2, and the continuous, gradual change when $n \geq 2$ can be explained within the framework of the Binek's model. We believe that this modified model will also be found to hold for the EB training effect in FM/AFM bilayers.

## References


[1] Xi H, White R M, Mao S, Gao Z, Yang Z and Murdock E 2001 *Phys. Rev. B* **64** 184416
[2] Pina E, Prados C and Hernando A 2004 *Phys. Rev. B* **69** 052402
[3] Brems S, Buntinx D, Temst K, Van Haesendonck C, Radu F and Zabel H 2005 *Phys. Rev. Lett.* **95** 157202
[4] Brems S, Temst K and Van Haesendonck C 2007 *Phys. Rev. Lett.* **99** 067201
[5] Polisetty S, Sahoo S and Binek C 2007 *Phys. Rev. B* **76** 184423
[6] Chan M K, Parker J S, Crowell P A and Leighton C 2008 *Phys. Rev. B* **77** 014420
[7] Mishra S K, Radu F, Dürr H A and Eberhardt W 2009 *Phys. Rev. Lett.* **102** 177208
[8] Shi Z, Du J, Chantrell R W, Mangin S and Zhou S M 2011 *Appl. Phys. Lett.* **98** 122507
[9] Keller J, Miltényi P, Beschoten B, Güntherodt G, Nowak U and Usadel K D 2002 *Phys. Rev. B* **66** 014431
[10] Binek C 2004 *Phys. Rev. B* **70** 014421
[11] Hoffmann A 2004 *Phys. Rev. Lett.* **93** 097203
[12] Qiu X P, Yang D Z, Zhou S M, Chantrell R, O'Grady K, Nowak U, Du J, Bai X J and Sun L 2008 *Phys. Rev. Lett.* **101** 147207
[13] Fulara H, Chaudhary S and Kashyap S C 2012 *Appl. Phys. Lett.* **101** 142408
[14] Shi Z, Qiu X P, Zhou S M, Bai X J and Du J 2008 *Appl. Phys. Lett.* **93** 222504
[15] Maity T, Goswami S, Bhattacharya D and Roy S 2013 *Phys. Rev. Lett.* **110** 107201
[16] Harres A and Geshev J 2011 *J. Phys.: Condens. Matter* **23** 216003
[17] Kaeswurm B and O'Grady K 2011 *Appl. Phys. Lett.* **99** 222508
[18] Ali M, Adie P, Marrows C H, Greig D, Hickey B J and Stamps R L 2007 *Nat. Mater.* **6** 70
[19] Yuan F T, Lin J K, Yao Y D and Lee S F 2010 *Appl. Phys. Lett.* **96** 162502
[20] Mydosh J A 1993 *Spin Glasses: An Experimental Introduction* (London, Washington, DC: Taylor & Francis Press) p. 105
[21] Rui W B, Hu Y, Du A, You B, Xiao M W, Zhang W, Zhou S M and Du J (unpublished)
[22] Nogués J and Schuller I K 1999 *J. Magn. Magn. Mater.* **192** 203
[23] Yuan F T, Yao Y D, Lee S F and Hsu J H 2011 *J. Appl. Phys.* **109** 07E148
[24] Ohldag H, Scholl A, Nolting F, Arenholz E, Maat S, Young A T, Carey M and Stöhr J 2003 *Phys. Rev. Lett.* **91** 017203
[25] Radu F and Zabel H 2008 *Magnetic Heterostructures, Springer Tracts in Modern Physics* **227** p. 109
[26] Su Y and Hu J 2012 *J. Appl. Phys.* **112** 043906
[27] Thomas S, Pookat G, Nair S S, Daniel M, Dymerska B, Liebig A, Al-Harthi S H, Ramanujan R V, Anantharaman M R, Fidler J and Albrecht M 2012 *J. Phys.: Condens. Matter* **24** 256004
[28] Xue X, Yuan X, Rui W, Xu Q, You B, Zhang W, Zhou S and Du J 2013 *Eur. Phys. J. B* **86** 1